IAI Journals.ASM.org

The Endothelin System Has a Significant Role in the Pathogenesis and Progression of *Mycobacterium tuberculosis* Infection

Andre F. Correa,[a,d] Alexandre M. Bailão,[b] Izabela M. D. Bastos,[a] Ian M. Orme,[c] Célia M. A. Soares,[b] Andre Kipnis,[d] Jaime M. Santana,[a] Ana Paula Junqueira-Kipnis[d]

Laboratório de Interação Parasito-Hospedeiro, Instituto de Biologia, Universidade de Brasília, Brasília, Brazil[a]; Laboratório de Biologia Molecular, Instituto de Ciências Biológicas, Universidade Federal de Goiás, Goiânia, Brazil[b]; Colorado State University, Fort Collins, Colorado, USA[c]; Instituto de Patologia Tropical e Saúde Pública, Universidade Federal de Goiás, Goiânia, Brazil[d]

Tuberculosis (TB) remains a major global health problem, and although multiple studies have addressed the relationship between *Mycobacterium tuberculosis* and the host on an immunological level, few studies have addressed the impact of host physiological responses. Proteases produced by bacteria have been associated with important alterations in the host tissues, and a limited number of these enzymes have been characterized in mycobacterial species. *M. tuberculosis* produces a protease called Zmp1, which appears to be associated with virulence and has a putative action as an endothelin-converting enzyme. Endothelins are a family of vasoactive peptides, of which 3 distinct isoforms exist, and endothelin 1 (ET-1) is the most abundant and the best-characterized isoform. The aim of this work was to characterize the Zmp1 protease and evaluate its role in pathogenicity. Here, we have shown that *M. tuberculosis* produces and secretes an enzyme with ET-1 cleavage activity. These data demonstrate a possible role of Zmp1 for mycobacterium-host interactions and highlights its potential as a drug target. Moreover, the results suggest that endothelin pathways have a role in the pathogenesis of *M. tuberculosis* infections, and ETA or ETB receptor signaling can modulate the host response to the infection. We hypothesize that a balance between Zmp1 control of ET-1 levels and ETA/ETB signaling can allow *M. tuberculosis* adaptation and survival in the lung tissues.

Tuberculosis (TB) remains a major global health problem. In 2012, an estimated 8.6 million people developed TB, and 1.3 million died from the disease (1). However, infection with *Mycobacterium tuberculosis* does not necessarily lead to TB disease. Less than 10% of immunocompetent individuals that are infected will progress toward active disease during their lifetimes (2). It is unknown if infected individuals are able to eradicate the bacteria following primary pulmonary infection. Although it is very well known that the adaptive immune Th1 and Th17 responses are important to control the disease, there is also evidence that suggests that early innate as well as adaptive immune defense mechanisms play a role in *M. tuberculosis* elimination. There still is little knowledge about the initial control of *M. tuberculosis*, although early gamma interferon (IFN-γ) production induced by cytokines such as interleukin-12 (IL-12) and tumor necrosis factor alpha (TNF-α) appears to be essential in initiating adequate immune responses to control the disease (3–7).

Proteases produced by bacteria have been implicated as important virulence factors (8), but only a few of these enzymes have been characterized in mycobacteria. Recently, an endopeptidase named Zmp1 with homology to human endothelin-converting enzyme 1 was described as being required for *M. tuberculosis* virulence and survival in macrophages (9), but a direct mechanism of action or a natural substrate remains unknown.

The endothelins are a family of 21-amino-acid vasoactive peptides, of which 3 distinct isoforms are known. Endothelin-1 (ET-1) is the most abundant and the best-characterized isoform. The endothelin precursor known as Big Endothelin (Big ET-1; 37 to 41 amino acids) is produced mainly by endothelial cells, and the vasoactive peptides are generated after cleavage by the endothelin-converting enzymes (ECE). Its activity contributes to endogenous tonic vasomotor maintenance by homeostatically balancing the vasodilation activity of NO. In addition, ET-1 also is produced by many cell types and released during various injurious stimuli, whereas atrial natriuretic peptide, prostacyclin, and nitric oxide (NO) inhibit its synthesis and release (10, 11). ET-1 binds to two distinct subtype receptors (ETA and ETB), which are presented in several cell types. Imbalances in these systems are associated with many diseases, including cardiovascular, pulmonary, and renal system diseases and carcinogenesis, and have effects on the pathophysiology of the immune system (12–14). In this regard, endothelin receptor antagonists (ERA) are being used already to treat some associated diseases (i.e., pulmonary hypertension), and several antagonists are under clinical trials (15).

Although many studies have investigated these physiological responses, there is little information linking endothelins and infectious diseases. In Chagas disease, for example, data provided evidence of a role for ET-1 in the pathogenesis of chronic cardiomyopathy (16), because ET-1 cooperatively activates *Trypanosoma cruzi*-mediated myocardial production of inflammatory mediators (17). Endothelin or ETR genes also are regulated during HIV (18–20) and other viral infections (21, 22) and correlate with

Received 7 July 2014 **Returned for modification** 5 August 2014
Accepted 19 September 2014
Published ahead of print 29 September 2014
Editor: B. A. McCormick
Address correspondence to Jaime M. Santana, jsantana@unb.br, or Ana Paula Junqueira-Kipnis, apkipnis@gmail.com.
Supplemental material for this article may be found at http://dx.doi.org/10.1128/IAI.02304-14.

doi:10.1128/IAI.02304-14

the severity of disease in patients with community-acquired pneumonia (23).

M. tuberculosis produces an endothelin-converting enzyme homologue, but to our knowledge no work has directly addressed if there is any impact on the endothelin pathway after *M. tuberculosis* infection; here, we show that Zmp1 from *M. tuberculosis* appears to have a role in host physiology, and this might contribute to *M. tuberculosis* pathogenicity. We report that Zmp1 from *M. tuberculosis* presents proteolytic activity that does not cleave Big ET-1 to release ET-1 peptide but is able to degrade ET-1. By applying endothelin receptor antagonism, we show a role for ET-1 in TB progression and inflammatory cell recruitment. In addition, we show here that ETR antagonism increased the numbers of lung lesions and increased bacterial burdens, whereas this could be reversed to some degree by an exogenous supply of ET-1.

MATERIALS AND METHODS

Mice. Specific-pathogen-free 5- to 8-week-old C57BL/6 female mice from the animal care facility of the Institute of Tropical Pathology and Public Health at UFG or inducible nitric oxide synthase knockout (iNOS-KO) mice from Universidade de São Paulo were maintained in isolators in biosafety level 3 (BL3) cabinets with water and food provided *ad libitum*. The temperature was maintained between 20 and 24°C, with the relative humidity set between 40 to 70% and with 12-h light/dark cycles. The use of mice was conducted in accordance with the guidelines of the Brazilian Society of Animal Science Laboratory (SBCAL/COBEA). The work was approved by CEUA-UFG (Comissão de Ética no Uso de Animais: Committee on the Ethics of Animal Experiments from Universidade Federal de Goiás), numbers 229/11 and 27/14.

Bacterial strains and growth conditions. *Mycobacterium tuberculosis* H37Rv was grown at 37°C in Middlebrook 7H9 broth or 7H11 agar supplemented with 10% oleic acid-albumin-dextrose (OAD), 0.5% glycerol, and 0.05% Tween 80. *Escherichia coli* strain XL1-Blue (Stratagene) was used for cloning and plasmid propagation. *E. coli* BL21 (Invitrogen) cells were used as expression-competent hosts. *E. coli* strains were maintained in Luria-Bertani (LB) medium at 37°C with or without the addition of kanamycin (50 μg/ml) or ampicillin (100 μg/ml) when required for plasmid selection. Solid medium was prepared by the addition of 1.5% agar to the LB medium.

Molecular cloning and recombinant protein expression. The *M. tuberculosis* Zmp1 gene (Rv0198c; http://genolist.pasteur.fr/TubercuList) was subcloned into PCR2.1 TOPO vector (Invitrogen) using a PCR-amplified product from the *M. tuberculosis* H37Rv genome. The recombinant PCR2.1 vector was digested to release the gene. After agarose gel elution, the released gene was ligated into the pET28a expression vector (Novagen). The recombinant pET28a construct containing the Zmp1 gene had its sequence checked with a BI 3130 capillary DNA sequencer (Applied Biosystems) and then was inserted into the expression host, *E. coli* BL21. Bacteria containing the recombinant expression vector were grown at 37°C. When the bacterial cells reached an optical density at 600 nm (OD_{600}) of 0.6, the expression of the fusion protein was induced by the addition of isopropyl-beta-D-thiogalactopyranoside (IPTG) to a final concentration of 0.5 mM, and the incubation continued at 20°C for 16 h. The bacterial cells were collected by centrifugation (10,000 × *g* for 5 min), and the cells were suspended in 4 ml of binding buffer (5 mM imidazole, 0.5 M NaCl, and 20 mM Tris-HCl, pH 7.9). After sonication, cell lysate was centrifuged (20,000 × *g* for 15 min), and the supernatant was applied onto a resin column (Novagen) charged with $NiSO_4$ and equilibrated with binding buffer. Proteins were eluted with a concentration gradient of imidazole (10 to 1,000 mM). Protein concentrations of the eluted fractions were determined by Bradford protein assay. Proteins were dialyzed against phosphate-buffered saline (PBS) and stored in 50% glycerol at −20°C. The purity of protein was analyzed by Coomassie-stained 12% SDS-PAGE gel.

Western blotting. H37Rv lysates and culture filtrate protein (CFP) were prepared from cultures grown in Sauton medium that does not have albumin enrichment present in Middlebrook media. Bacterial culture was grown in 200 ml of Sauton liquid media to late log phase. Bacteria were pelleted by centrifugation at 2,000 × *g* for 20 min. The bacterial pellet was used to prepare H37Rv lysates by sonication. Supernatant was transferred to a fresh tube and centrifuged again before being filtered through a 0.2-μm filter unit. Supernatant was concentrated by protein acetone precipitation (24) and solubilized in SDS-PAGE sample buffer. Samples were resolved by 12% SDS-PAGE and transferred to a nitrocellulose membrane. Membranes were blocked in 5% nonfat powdered milk in PBS and probed with the anti-rZmp1 polyclonal serum produced in mice, followed by the anti-mouse IgG-alkaline phosphatase secondary antibody (Sigma-Aldrich). Antigen-antibody complex was detected via 5-bromo-4-chloro-3-indolylphosphate-nitroblue tetrazolium liquid substrate system (Sigma-Aldrich).

Enzyme activity assay. The endopeptidase activity of rZmp1 was assayed by incubating 100 ng of purified enzyme with 20 μM ECE-1 fluorescent substrate (Sigma-Aldrich) in PBS to a final volume of 100 μl. Substrate hydrolysis was measured fluorometrically with a SpectraMax M5 microplate reader with SoftMax Pro Data Acquisition & Analysis Software (Molecular Devices) for 15 min at 25°C. Briefly, 100 μM Big ET-1 (Sigma-Aldrich) or 100 μM ET-1 (Sigma-Aldrich) was incubated with or without 100 ng purified rZmp1 preparations in 100 μl PBS containing 5 μM $ZnSO_4$. Samples were incubated at 37°C for 1 to 4 h, and the reactions were stopped by cooling of the samples to −80°C. The cleavage of the peptides was detected by matrix-assisted laser desorption-ionization (MALDI) or liquid chromatography-electrospray ionization (LC-ESI) sources with quadrupole time-of-flight analysis (Q-TOF) mass spectrometry (MS) (Synapt; Waters). Samples were spotted (2 μl) in a target plate and dried at room temperature. The peptides next were covered with 10 mg/ml of α-cyano-4-hydroxyciannamic acid in 50% acetonitrile and 0.1% trifluoroacetic acid and dried. The mass spectra were obtained in positive reflectron mode on a MALDI-Q-TOF mass spectrometer (Synapt). For LC-ESI-Q-TOF MS, the sample aliquots were diluted in water (1:10). The peptides were separated in a nanoACQUITY (Waters) system by using an analytical column (1.7-μm BEH130 C_{18}; 100 μm by 100 μm) in an acetonitrile gradient from 7% to 40% during 60 min. The spectra were analyzed using MassLynx software (Waters).

***M. tuberculosis* infection and treatment with ET-1 and ETR antagonists.** Mice were given, by intranasal instillation, 100-μl doses containing 1 μM solutions of BQ123 (ETA antagonist; $n = 4$), BQ788 (ETB antagonist; $n = 4$), ET-1 ($n = 4$; Sigma-Aldrich), or vehicle (0.2% dimethylsulfoxide [DMSO] in PBS; $n = 4$) three times a week on alternate days for 4 weeks. After the first week of treatment, the mice were infected with 10^4 *M. tuberculosis* H37Rv intranasally. As a control, 100 μl of saline was given ($n = 4$). The experiments were repeated three times. To enumerate the viable bacteria in the mouse lungs, animals were euthanized 21 days after infection. The anterior and middle right lung lobes were removed and homogenized in 0.05% Tween 80 in PBS, and the tissue homogenates were serially diluted in PBS and plated in duplicate onto Middlebrook 7H11 agar. The colonies were counted after 3 to 4 weeks of incubation at 37°C, and the results are presented as the mean $\log_{10}$ CFU per mouse.

Histopathology. The posterior left lung lobe was excised from all animals, stored in 10% formalin, and then embedded in paraffin at different times. From the paraffin-embedded tissue blocks, 3-μm sections were prepared and stained with hematoxylin and eosin (H&E). The H&E-stained lung sections were photographed using a microscope at ×40 magnification, and the area of lesions in the lung was determined using the measurement tool in AxioVision software (Carl Zeiss). Three photographs were taken by lung lobe per mouse. Total lesion area was calculated by the sum of all areas of lesions in a lung section per mouse.

Preparation of BAL fluid and lung cell suspensions. Cells were obtained by slight modification of the method previously described (25). Mice were euthanized, and the pulmonary cavities were opened. After

severing the descending aorta, the blood in the lungs was cleared by perfusion through the heart right ventricle with 5 ml of PBS containing 50 U/ml of heparin (Sigma-Aldrich) until the lungs became whitish. Using an 18-gauge needle, the trachea was cannulated and 1 ml of ice-cold 5 mM EDTA in PBS was slowly injected into the lungs and then withdrawn. This procedure was repeated twice, and a total of 1.5 ml of bronchoalveolar lavage (BAL) fluid was collected. To obtain lung cell populations, the right bottom lobe was aseptically removed and cut into small pieces. The dissected tissue was incubated in RPMI medium 1640 (Gibco) supplemented with 1% glutamine (Sigma-Aldrich), 1% nonessential amino acids (Sigma-Aldrich), 1 mM sodium pyruvate (Sigma-Aldrich), and 1% penicillin-streptomycin (Sigma-Aldrich) containing collagenase XI (0.7 mg/ml; Sigma-Aldrich) and type IV bovine pancreatic DNase (30 mg/ml; Sigma-Aldrich) during 30 min at 37°C. Ten ml of RPMI medium containing 10% fetal bovine serum (FBS) (cRPMI) was added, and digested lungs were further disrupted by gently pushing the tissue through a 70-μm nylon screen. The single-cell suspension then was washed and centrifuged at 1,000 × *g*. To lyse contaminating red blood cells, the cell pellet was incubated during 5 min at room temperature with 2 ml of Gey's solution (NH_4Cl and $KHCO_3$). Cells then were washed with RPMI and resuspended in 1 ml of cRPMI. The amount of 10^5 cells from BAL fluid and 10^6 from lung were Fc blocked with 10% mouse serum and then stained for 30 min at 4°C with directly conjugated antibodies using the BD Cytofix/Cytoperm kit according to the manufacturer's instructions. The monoclonal antibodies specific for CD11c (N418), CD11b (M1/70), Gr1 (RB6-8C5), and CD14 (Sa2-8) were purchased from BD Bioscience or eBioscience as direct conjugates to fluorescein isothiocyanate (FITC), phycoerythrin (PE), peridinin chlorophyll protein (PerCP), PerCP-cyanine 5.5, or allophycocyanin. Cell acquisition was performed with a dual-laser flow cytometer (FACSCalibur and FACSVerse; BD Biosciences). The data were analyzed using FlowJo software (TreeStar).

Statistical analysis. Statistical significance between groups was determined by the two-tailed unpaired Student's *t* test or one-way analysis of variance (ANOVA) with Dunnett's posttest using Prism software, version 5.03 (GraphPad).

RESULTS

Zmp1, a secreted mycobacterial endopeptidase. Prior to testing endopeptidase activity, the Zmp1 enzyme from *Mycobacterium tuberculosis* was cloned into the prokaryotic expression vector pET28a. The recombinant protein (rZmp1) was expressed and purified by nickel affinity chromatography under nondenaturing conditions. SDS-PAGE analyses revealed a strong band, with high purity, corresponding to the expected size of approximately 76 kDa (Fig. 1A). The native protein in the cell extract of H37Rv and also in the culture filtrate proteins (CFP) was identified by Western blotting using anti-rZmp1 polyclonal serum produced in mice (Fig. 1B). The presence of extracellular Zmp1 was not due to nonspecific bacterial lysis, because the culture supernatants were probed for a mycobacterial cytoplasmic enzyme, Rv2213, which was not detected (see Fig. S1 in the supplemental material). Thus, despite having no signal sequence (9), protein Zmp1 was secreted by the bacterium. In order to evaluate if the recombinant protein remained functional, ECE-1 fluorescent substrate was used to show that the enzyme was active (Fig. 1C) and lost its activity when subjected to high temperatures.

Zmp1 does not generate ET-1 from Big ET-1. ECE-1 is involved in proteolytic processing of Big ET-1 precursors, with an estimated mass of 4,281 Da, to produce a biologically active ET-1 peptide with a mass of 2,491 Da. To test whether Zmp1 mediates this same activity, the active recombinant protein was incubated with the Big ET-1 peptide, and the reaction product was analyzed by mass spectrometry. The spectrogram of intact peptide showed

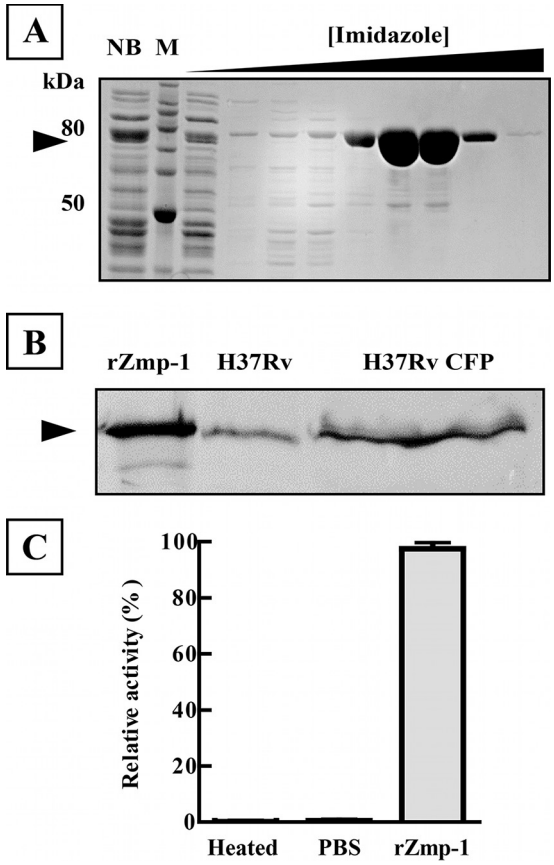

FIG 1 Zmp1 characterization. (A) Purification of recombinant Zmp1 (rZmp1). IPTG-induced rZmp1 was purified by nickel affinity chromatography. The resin unbound fraction (NB), molecular mass marker (M), and elution with increasing imidazole concentrations ([Imidazole]) were analyzed by 12% reducing SDS-PAGE and stained with Coomassie brilliant blue. (B) Localization of Zmp1 by immunoblot analysis. For lane rZmp1, H37Rv total cell lysate (H37Rv) and H37Rv culture filtrate proteins (H37Rv CFP) were probed with rZmp1 polyclonal mouse antiserum. Arrowheads indicate the Zmp1 position at 76 kDa. (C) Activity of rZmp1. One hundred ng of purified rZmp1, rZmp1 preheated for 10 min at 100°C (heat), or PBS was incubated with 20 μM ECE-1 substrate. Data shown represent the means ± standard errors of the means (SEM) of relative activity to maximum fluorescence emission ($n = 3$).

a peak mass/charge (*m/z*) ratio of 4,281, which matches the expected Big ET-1 mass (Fig. 2A). Even after prolonged incubation, the enzyme showed low activity, and the peptide remained largely intact at 4,281 Da. Further analyses showed that no fragment was observed by MALDI-Q-TOF MS evaluation (Fig. 2B). In addition, using LC-ESI-Q-TOF MS, no peptide Big ET-1 cleavage with ET-1 release was observed (see Fig. S2 in the supplemental material).

Zmp1 cleaves endothelin peptide. Since the enzyme was not able to generate ET-1 by Big ET-1 cleavage, we then investigated whether rZmp1 instead is involved in the degradation of the mature peptide (ET-1). By LC-ESI-TOF MS analysis, the intact endothelin peptide showed a peak with a retention time of 36 min, 831 *m/z* three times protonated (peptide charged with three H^+ ions), and 1,246 *m/z* with two H^+ molecules, which corresponds to the expected mass of 2,491 Da for ET-1 (Fig. 3A). After incubation of ET-1 with rZMp1, the peptide was hydrolyzed, resulting in peptides of 1,470 and 431 Da. Therefore, there are at least two cleavage sites between amino acid residues Y13-F14 and D18-I19 (Fig. 3B).

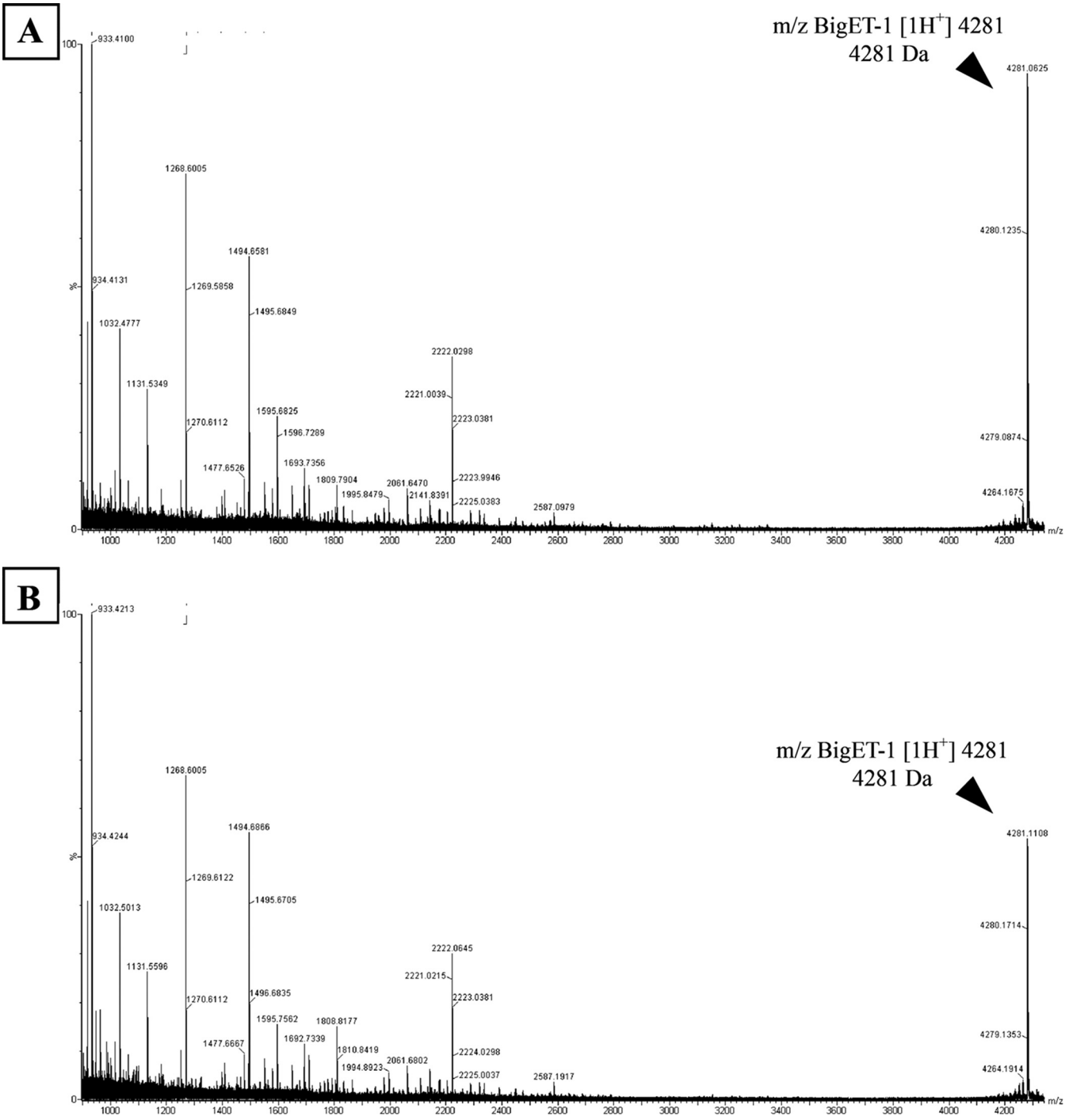

FIG 2 Hydrolysis of Big Endothelin-1 by rZmp1. (A) MALDI-Q-TOF spectrum of Big Endothelin-1 peptide (Big ET-1). (B) MALDI-Q-TOF spectrum of rZmp1-hydrolyzed Big ET-1 peptide. The arrowheads indicate the peaks of interest, with 4,281 *m/z* corresponding to Big ET-1 with a mass of 4,281 Da.

Blocking endothelin receptor signaling during *M. tuberculosis* infection causes increased severity of lesions and bacterial loads in the lungs. Considering the production and secretion by *M. tuberculosis* of an enzyme able to degrade endothelin, which might affect lung capillary integrity, we looked to see the consequences of lower ET-1 levels during *M. tuberculosis* infection in the lungs. For this, we used the specific endothelin receptor antagonists (ERA) BQ123 (ETA antagonist) and BQ788 (ETB antagonist), which were administered by intranasal instillation, reducing potential systemic effects. The administration of endothelin receptor antagonists in naive mice challenged with saline did not alter lung morphology (Fig. 4A and B). However, when mice previously infected with *M. tuberculosis* were treated with ERA, a significant increase in pulmonary lesions caused by infection was

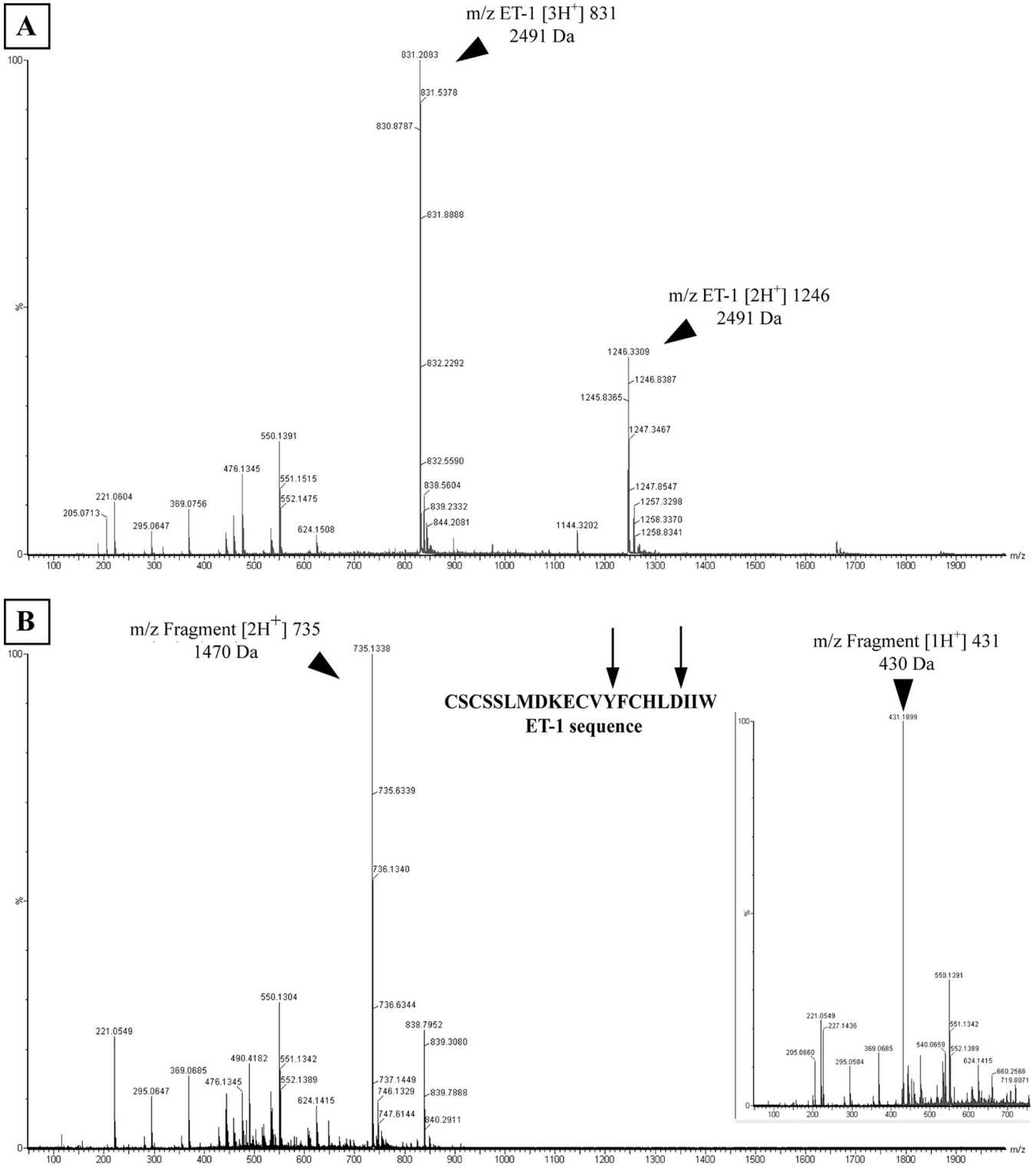

FIG 3 Hydrolysis of ET-1 by rZmp1. (A) LC-ESI-Q-TOF-MS spectrum of ET-1 peptide. Peaks of 831 *m/z* three times protonated (triply charged ion, $3H^+$) and 1,246 *m/z* two times, corresponding to ET-1 at 2,491 Da. (B) LC-ESI-Q-TOF-MS spectrum of rZmp1-hydrolyzed ET-1 peptide. Peak of 735 *m/z* two times protonated ($2H^+$) with a retention time of 9.47 min and corresponding to a 1,470-Da fragment. The inset shows a peak with a 18.18-min retention time and 431 *m/z* with one H^+. Arrows over ET-1 sequence indicate cleavage sites for rZmp1. The arrowheads indicate the peaks of interest.

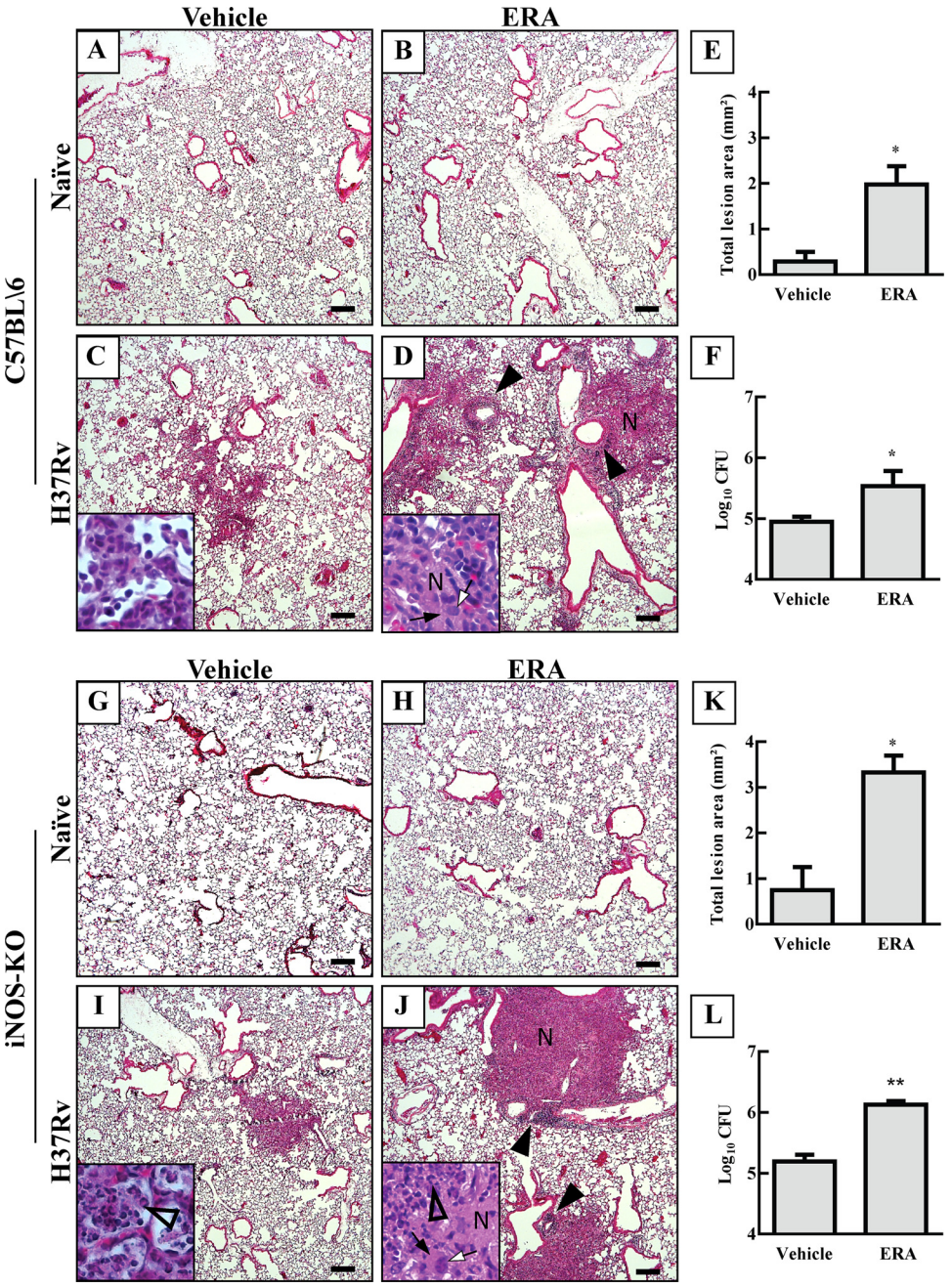

FIG 4 Effects of endothelin receptor antagonism in C57BL/6 (A to F) and iNOS-KO (G to L) mice during early *M. tuberculosis* infection. (A to D and G to F) Representative lung (posterior left lobe) photomicrographs of mice treated with vehicle (A and G) or with ERA (BQ788 and BQ123) (B and C) after 21 days of treatment and *M. tuberculosis* H37Rv-infected mice treated with vehicle (C and I) or ERA (D and J) at 21 days postinfection and under treatment. Black arrowheads indicate lymphocytic infiltrate. Insets show the magnification of lesion area with necrosis (N), cells with large lateral nuclei (white arrow), and very long cytoplasmic processes (black arrow) and neutrophils (open arrowhead). Scale bars correspond to 200 μm. (E and K) Results of the quantification of the inflammatory lesion area sizes (left bottom lobe) from C57BL/6 (E) and iNOS-KO (K) mice infected with *M. tuberculosis* and treated with vehicle or ERA (BQ123 and BQ788). (F and L) Bacterial burden of lung (anterior and middle right lobes) from C57BL/6 (F) and iNOS-KO (L) mice infected with *M. tuberculosis* H37Rv at 21 days postinfection, treated with vehicle or ERA. Data shown represent means ± SEM, $n = 3$. *, $P < 0.05$; **, $P < 0.01$ (both by *t* test).

observed (1.975 mm^2) compared to the level for the infected (0.288 mm^2) group treated with vehicle (Fig. 4E). The main histological differences were bronchiolar and perivascular infiltrates with high concentrations of lymphocytes (Fig. 4D), with regions of necrosis and the presence of cells with large nuclei and bulky cytoplasm (Fig. 4D, inset) present in infected mice that received the antagonist treatment. These alterations were not observed in the group treated with vehicle alone (Fig. 4C). In addition, there was a significant increase in the bacterial load (~0.5 log) in the lungs of mice that received treatment with antagonists (Fig. 4F).

The ETRs' antagonism effects in early *M. tuberculosis* infection are iNOS independent. It has been well described in the lit-

erature that a regulatory balance exists between nitric oxide and endothelin (26) and that, during the inflammatory process, such as in the lungs, the main source of NO is provided by iNOS (27). Thus, the effect of the ERA treatment in *M. tuberculosis*-infected mice could be mediated by changes in the expression and activity of iNOS. To analyze this possibility, iNOS knockout mice were treated with ERA and infected with *M. tuberculosis*. The animals were evaluated 21 days postinfection. At this time point, iNOS knockout mice (iNOS-KO) showed lung abnormalities similar to those of wild-type mice (C57BL/6). There were no pathological changes in the lung of mice treated with ERA (Fig. 4H) compared to the vehicle group (Fig. 4G). Again, endothelin receptor antagonism increased lung inflammatory reactions to *M. tuberculosis* infection that changed from a lesion size of 0.745 mm^2 in the vehicle group to 3.327 mm^2 in the ERA-treated animals (Fig. 4K). Perivascular and peribronchial inflammatory infiltrates (Fig. 4J), increased areas of necrosis, and the presence of cells with large nuclei and long cytoplasmic processes were observed in ERA-treated inflammatory reactions (Fig. 4J, inset). Large numbers of neutrophils also were observed. Nonetheless, this difference was not caused by ERA treatment (Fig. 4I and J, insets). The increased bacterial load (~0.9 log) caused by ERA treatment also was observed in the knockout mouse group (Fig. 4L).

Different cell populations expressing Gr1 are increased by ETR antagonism during *M. tuberculosis* infection. Since the lesions and bacterial burden observed in the ERA-treated *M. tuberculosis*-infected mice were not associated with iNOS activity, we hypothesized that ERA treatment could affect the phenotype or cell migration to the infected lungs, consequently modulating the immune response by increasing suppressor cells and increasing the bacterial load. Mouse cells with a $Gr1^+$ myeloid-derived suppressor cell (MDSC) phenotype may have the morphology of various cell types, such as granulocytes, dendritic cells, monocytes, or macrophages, that expand during cancer, inflammation, and infection and that have a remarkable ability to suppress T-cell responses (28). Thus, we decided to question whether these cells were involved in the ERA treatment outcome. To access this heterogeneous population using flow cytometry, cells were defined according to the expression of the Gr1 marker. Cells expressing low levels of Gr1 ($Gr1^{low}$) were gated as R1, cells expressing intermediate levels ($Gr1^{int}$) were gated as R2, and cells expressing high levels of the Gr1 marker were defined as $Gr1^{high}$ and gated as R3 (see Fig. S3 in the supplemental material).

Although ERA treatment alone did not change the proportions of $Gr1^+$ cells in the lungs of C57BL/6 or iNOS-KO mice (Fig. 5), the infection with *M. tuberculosis* affected only some of these cell populations, depending on the mouse background. *M. tuberculosis* infection alone did not change the population of $Gr1^{low}$ cells in C57BL/6 mice, whereas ERA-treated animals showed a decrease in the percentage of $Gr1^{low}$ cells compared to the naive vehicle-treated mice (Fig. 5A). In the absence of NO, *M. tuberculosis* infection causes a small decrease of $Gr1^{low}$ cells in both vehicle- and ERA-treated mice (Fig. 5B). The association of ERA treatment and infection directly affects the $Gr1^{int}$ cells, because C57BL/6 and iNOS-KO mice showed an increase in this population, almost tripling its proportion in C57BL/6 mice (Fig. 5C and D). In order to further characterize those cells, the $Gr1^{low}$ cells were evaluated for the expression of CD11c and CD14, and it was observed that these cells were CD11c and CD14 positive, which probably identifies them as monocytes and/or macrophages. The $Gr1^{int}$ cells expressed low levels of CD14 and were negative for CD11c, which indicates the presence of MDSC in lungs of ERA-treated mice (see Fig. S4 in the supplemental material). Basically the same changes were observed in cells obtained from BAL fluid of these mice, with the exception of $Gr1^{low}$ cells, which had no significant changes (see Fig. S5).

Additionally, ERA treatment also enhanced the $Gr1^{high}$ cells in C57BL/6-infected mice (Fig. 5E), while in iNOS-KO mice the infection induced an increase in these populations that was further improved with ERA treatment (Fig. 5F). This cell phenotype marker was associated with neutrophils (i.e., expressing low to intermediate levels of CD14 and CD11c negative) (see Fig. S4 in the supplemental material), which were observed at high levels in iNOS-KO mice (Fig. 4, insets).

Endothelin-1 reduces the progression of lesion severity and plays different roles through ETA and ETB receptors. As noted above, the ETR antagonism caused changes in the response to *M. tuberculosis*. Thus, we decided to analyze the consequences of increased endothelin-1 during infection and the role of each receptor separately. For this, infected C57BL/6 mice were supplied with exogenous endothelin-1 peptide, while BQ123 (ETA antagonist) and BQ788 (ETB antagonist) were administered separately, all by intranasal instillation. Lung *M. tuberculosis* infection at 21 days postinfection presented some perivascular/peribronchial inflammatory foci and moderate alveolar damage area (Fig. 6A). Further, infected mice treated with ET-1 showed a reduction in the number and size of the inflammatory reactions, with little alveolar damage compared to the mice treated with vehicle (Fig. 6B and E). Although ET-1-treated mice presented the best histological findings, no difference was seen in the bacterial loads in the lungs compared to the controls (Fig. 6F). The group that received the ETA antagonist BQ123 showed an increase of lung lesion area with more intense inflammatory foci, diffuse alveolar damage, pulmonary edema, and some necrosis (Fig. 6C and E), but again there was no increase in the bacterial load (Fig. 6F). In contrast, blockade of ETB by treatment with BQ788 had no effect on the number or size of lesions (Fig. 6D and E) compared to *M. tuberculosis*-infected animals treated with vehicle; however, we did observe an increase in lung CFU in these animals (Fig. 6F). Simultaneous ETA and ETB antagonism (ERA) induced an increase in lesion area and bacterial load in the lungs of infected mice (Fig. 4 and 6E and F).

DISCUSSION

In this study, we characterized Zmp1, a metalloprotease belonging to the M13 family, as an enzyme secreted by *M. tuberculosis* that is able to cleave ET-1. In mass spectrometry analyses, no ET-1 release from Big ET-1 was observed after Zmp1 incubation. In contrast, Zmp1 efficiently hydrolyzed the mature ET-1 peptide. We then showed that the blockade of ET-1 activity by antagonism during *M. tuberculosis* infection resulted in an increased number and severity of lung lesions, as well as increases in bacterial burden. These events could be reduced somewhat by the exogenous delivery of the ET-1 peptide.

Zmp1 was previously described in *M. tuberculosis* (9, 29) and in other bacteria, including *Streptococcus parasanguis* (30, 31) and *Porphyromonas gingivalis* (32), as a protease with activity on small biologically active peptides, but no activation on endothelins was seen. In *P. gingivalis*, the protease showed activity against Big Endothelin (33), but the results were controversial, and ET-1 generation could not be confirmed by enzyme-linked immunosorbent

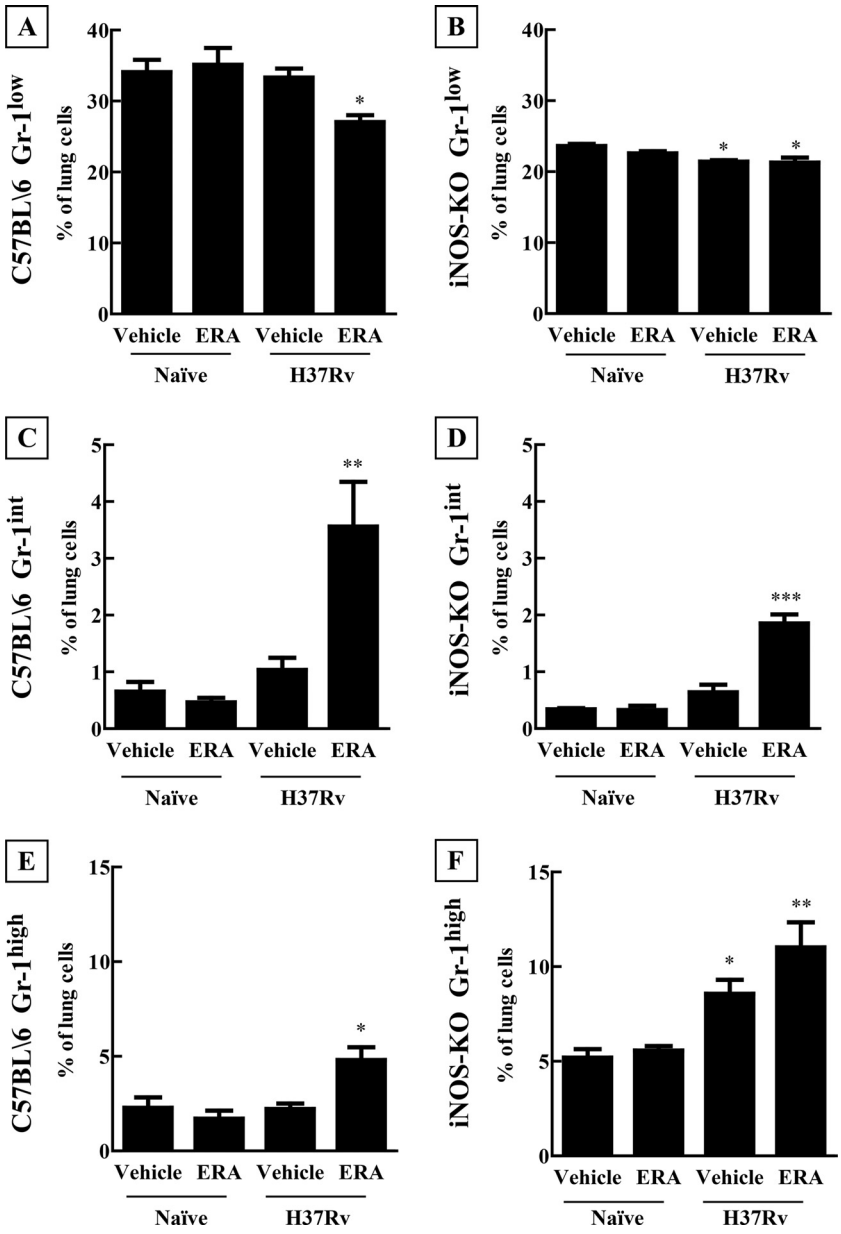

FIG 5 Cellular changes in the lungs by ET-1 receptor blockade during early *M. tuberculosis* infection. Shown are the percentages of lung cells in uninfected (naive) or *M. tuberculosis* (H37Rv)-infected mice at 21 days postchallenge with vehicle or endothelin receptor antagonist BQ123 and BQ788 (ERA) treatment. Proportion of $Gr1^{low}$ cells in C57BL/6 (A) or iNOS-KO (B) mice, $Gr1^{int}$ cells from C57BL/6 (C) or iNOS-KO (D), and $Gr1^{high}$ cells as a percentage in C57BL/6 (E) or iNOS-KO (F) mice. Data shown represent means ± SEM, $n = 3$. *, $P < 0.05$; **, $P < 0.01$; ***, $P < 0.001$; differences from the naive vehicle treatment group were determined by one-way ANOVA with Dunnett's posttest.

assay (ELISA). Here, we found that the mycobacterial enzyme Zmp1 does not act as an ECE that converts Big ET-1 into ET-1 mature peptide (Fig. 2) but instead appears to act by hydrolyzing ET-1 (Fig. 3). Like other oligopeptidases (34), Zmp1 seems to be active on peptides with less than 30 amino acids, and this preference for peptides also is confirmed by the solved X-ray crystallographic structure of Zmp1, which reveals that the active site is located at the bottom of a hydrophobic channel, likely impairing access of large macromolecular substrates in the proximity of the reaction center (35), which may explain its low activity against the large Big ET-1 peptide. Cleavage sites found in the ET-1 peptide (Fig. 3) were in accordance with the previously identified cleavage pattern for Zmp1 on other substrates (29), showing a preference for phenylalanine and isoleucine amino acid residues at the P1′ position. In addition, the C-terminal as well as the N-terminal intramolecular loop structure is especially important for endothelin activity; thus, an enzymatic system might exist as a physiological mechanism for converting ET-1 to biologically inactive forms (36, 37). Further, proteases of pathogenic bacteria, fungi, and protozoa have been described to hydrolyze many human bioactive peptides (38–40).

A previous report has indicated that Zmp1 mediated the arrest

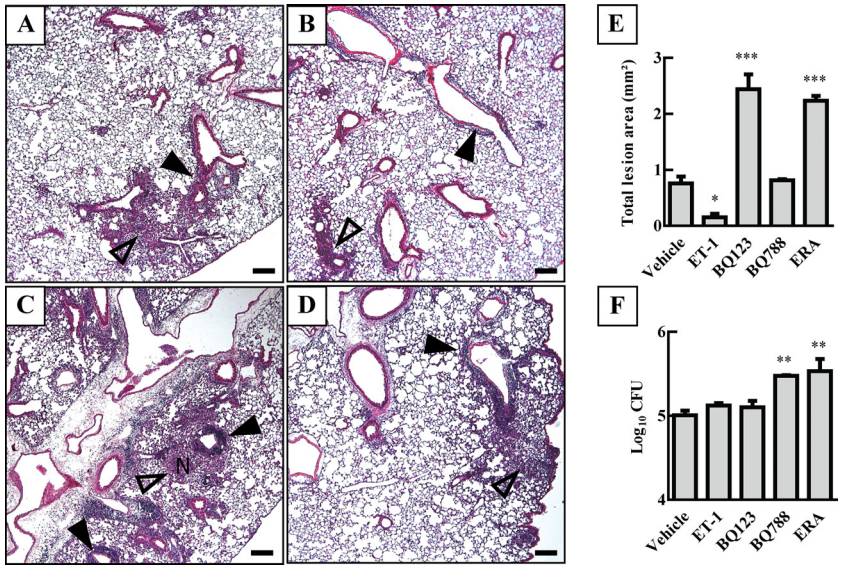

FIG 6 ET-1 promotes different responses through A and B receptors during *M. tuberculosis* infection. (A to D) Representative lung sections (left bottom lobe) with HE stain of *M. tuberculosis*-infected mice treated with vehicle (A), ET-1 (B), ETA antagonist BQ123 (C), or ETB antagonist BQ788 (D) at 21 days postinfection and under treatment. Indicated are perivascular/peribronchial inflammatory infiltrate (black arrowhead), alveolar damage (open arrowhead), and lesion area with necrosis (N). Scale bars represent 200 μm. Also shown are results of the quantification of the inflammatory lesion area sizes (E) and bacterial burden of lung (anterior and middle right lobes) from infected mice treated with vehicle, ET-1, BQ123, BQ788, and ERA (BQ123 and BQ788) at 21 days postinfection and under treatment (F). Data shown represent means ± SEM, $n = 3$. *, $P < 0.05$; **, $P < 0.01$; ***, $P < 0.001$; differences from vehicle treatment were determined by one-way ANOVA with Dunnett's posttest.

of phagosome maturation (41), and genetic inactivation of the Zmp1 gene generated an attenuated strain that triggered the activation of the inflammasome, resulting in increased IL-1β secretion normally preempted in the *M. tuberculosis* wild-type strain (9). In addition, ET-1 is an important mediator of IL-1β inflammatory response (42). Complementary to our findings for enzymatic peptide hydrolysis (Fig. 3), these data suggest a role for Zmp1 in the mycobacterial virulence that may involve ET-1 signaling.

As observed here, when mice treated with BQ123 were infected with *M. tuberculosis*, increased lung lesions occurred, which may be explained because the blocked receptor (ETA) is a primary vasoconstrictor and a growth-promoting receptor (13). Thus, ETA blocking may have promoted vasodilation that facilitated the perfusion and infiltration of inflammatory cells, inducing more tissue damage during *M. tuberculosis* infection (Fig. 4 and 6). However, this inflammatory process could not control *M. tuberculosis* infection, so no bacterial load decrease was observed in the lung (Fig. 6).

ERA treatment increased the number of $Gr1^{high}$ cells. Neutrophils (Fig. 4 and 5) were present at higher levels during the chronic stage of murine tuberculosis (43), as were $Gr1^{int}$ cells, suggesting a $Gr1^{+}$ myeloid-derived suppressor cell phenotype. Based on previous experiments showing that $Gr1^{int}$ MDSC cells diminished the T-cell protective responses in a murine TB model (44, 45), our results corroborate these findings to a certain degree, particularly because *M. tuberculosis*-infected animals treated with ERA showed a diminished ability to control the infection. Further, ETR signaling could modulate recruiting or phenotype changes of these MDSC cells.

In contrast, ETB antagonism led to higher bacterial burdens but no overt histological changes (Fig. 6). These responses could be explained by the distinct ETR subtype functions in vascular and inflammatory responses, because both ETA and ETB receptors act on vascular smooth muscle and mediate ET-1-induced vasoconstriction (46). However, in pulmonary endothelium, ETB receptors mediate the generation of NO or the opening of ATP-sensitive potassium channels, and NO promotes vasodilation (47, 48). Thus, ETB antagonism could induce vasoconstriction and prevent inflammatory cell infiltration in lung tissue. In addition to the vascular tone functions of ETB in the lungs, this receptor also acts as a clearance receptor, capturing blood-circulating ET-1 and leading to the clearance of the peptide in pulmonary tissue (47, 49). In immune responses, results with knockout mice (50) and ETR antagonists (51) suggest that the proinflammatory effects of ET-1 are mediated by the ETB receptor, including fever (42, 52). Therefore, BQ788 can act as an anti-inflammatory mediator by directly blocking ETB receptor proinflammatory effects and also decreasing lung uptake of ET-1 from the circulation, leading to lowered ET-1 lung activity and, in turn, allowing increasing bacterial burdens in the lung tissues. In addition, we have demonstrated that the exogenous administration of ET-1 can reduce *M. tuberculosis* infection lesions (Fig. 6). On the other hand, using whole-genome microarray gene expression analysis, ET-1 gene expression was associated with the severity of *M. tuberculosis* infection (53). Whether the increase of ET-1 expression was to counteract the effect of the *M. tuberculosis* inflammatory response or is a consequence of the infection needs to be further investigated.

Similarities in the responses of iNOS knockout and C57BL/6 mice to ERA (Fig. 4 and 6) corroborate the classic ET-1 signaling pathway, where ET-1 stimulates NO production by activation of endothelial NO synthase (eNOS) instead of iNOS (54, 55). However, iNOS knockout-infected mice showed increased neutrophil

content (Fig. 4, insets, and 5) and a tendency for higher numbers of CFU and larger lesions (Fig. 4). ERA significantly increased the neutrophil population during *M. tuberculosis* infection only in wild-type mice (Fig. 5). iNOS deficiency in septic mice facilitated the infiltration of neutrophils into pulmonary tissue from the pulmonary microvasculature, and the transendothelial neutrophil migration was attenuated by the specific presence of iNOS in neutrophils (56). In our murine tuberculosis model, iNOS also appears to play a role in neutrophil infiltration and endothelin signaling that specifically affects the neutrophil iNOS. Bacterial burden and lung injury pattern in iNOS-KO mice agree with the literature data from murine models of tuberculosis, showing a more susceptible phenotype (57). However, the antimycobacterial activity of NO *in vivo* and whether NO is critically involved in the host defense against *Mycobacterium tuberculosis* in humans is controversial (27). Nevertheless, our data suggest a vascular mechanism of control for *M. tuberculosis*. Thus, it may be that NO acts in this *M. tuberculosis* control mechanism and in neutrophil migration rather than as a bactericidal agent. Further, ET-1 could be involved in decreased oxygen tension or hypoxia described in granulomas undergoing caseous necrosis and characterized by a lack of vascularity in human tissue (58). Therefore, more studies must be carried out in other models, because hypoxia usually is not found in the TB mouse models (59, 60).

In summary, our results show that *M. tuberculosis* produces and secretes an enzyme with ET-1 cleavage activity and may act as a virulence factor. These data demonstrate a possible role of Zmp1 in mycobacterium-host interactions. Moreover, endothelin pathways have a role in the pathogenesis of *M. tuberculosis* infections, and ETA or ETB receptor signaling can modulate the host response against bacilli. Thus, a balance between Zmp1 control of ET-1 levels and ETA/ETB signaling can allow *M. tuberculosis* adaptation and survival in lung tissue.

ACKNOWLEDGMENTS

This work was supported by CNPq (Conselho Nacional de Desenvolvimento Científico e Tecnológico-Brasil; grant numbers 307186/2013-0 and 301976/2011-2), CNPq-Pronex-DF, FAPDF (Fundação de Apoio à Pesquisa do Distrito Federal), Finep (Financiadora de Estudos e Projetos), FAPEG (Fundação de Amparo à Pesquisa do Estado de Goiás), and CAPES/COFECUB. A.F.C. received a Ph.D. fellowship from CAPES (Coordenação de Aperfeiçoamento de Pessoal de Nível Superior).

The funders had no role in study design, data collection and analysis, decision to publish, or preparation of the manuscript.

We thank the flow cytometry core facility of Associação de Combate ao Câncer do Estado de Goiás, Aline Carvalho Batista for use of the histopathology core facility at Faculdade de Odontologia from Universidade Federal de Goiás and LACEN-DF (Laboratório Central de Saúde Pública do Distrito Federal). We also thank Simone Fonseca from Universidade Federal de Goiás for critically revising the manuscript.

A.F.C., J.M.S., and A.P.J.-K. conceived and designed the experiments. A.F.C. and A.P.J.-K. performed the experiments. A.F.C., A.K., I.M.O., and A.P.J.-K. analyzed the data. A.P.J.-K., A.M.B., I.M.D.B., A.K., J.M.S., and C.M.A.S. contributed reagents/materials/analysis tools. A.F.C. wrote the manuscript draft. All authors critically revised the manuscript.

REFERENCES

1. **WHO.** 2013. Global tuberculosis report 2013. World Health Organization, Geneva, Switzerland. http://www.who.int/tb/publications/global_report/en/.
2. **Barry CE, Boshoff HI, Dartois V, Dick T, Ehrt S, Flynn J, Schnappinger D, Wilkinson RJ, Young D.** 2009. The spectrum of latent tuberculosis: rethinking the biology and intervention strategies. Nat. Rev. Microbiol. **7:**845–855. http://dx.doi.org/10.1038/nrmicro2236.
3. **Ottenhoff THM, Kaufmann SHE.** 2012. Vaccines against tuberculosis: where are we and where do we need to go? PLoS Pathog. **8:**e1002607. http://dx.doi.org/10.1371/journal.ppat.1002607.
4. **Kamijo R, Le J, Shapiro D, Havell EA, Huang S, Aguet M, Bosland M, Vilcek J.** 1993. Mice that lack the interferon-gamma receptor have profoundly altered responses to infection with Bacillus Calmette-Guérin and subsequent challenge with lipopolysaccharide. J. Exp. Med. **178:**1435–1440. http://dx.doi.org/10.1084/jem.178.4.1435.
5. **Keane J, Gershon S, Wise RP, Mirabile-Levens E, Kasznica J, Schwieterman WD, Siegel JN, Braun MM.** 2001. Tuberculosis associated with infliximab, a tumor necrosis factor alpha-neutralizing agent. N. Engl. J. Med. **345:**1098–1104. http://dx.doi.org/10.1056/NEJMoa011110.
6. **Altare F, Durandy A, Lammas D, Emile JF, Lamhamedi S, Le Deist F, Drysdale P, Jouanguy E, Döffinger R, Bernaudin F, Jeppsson O, Gollob JA, Meinl E, Segal AW, Fischer A, Kumararatne D, Casanova JL.** 1998. Impairment of mycobacterial immunity in human interleukin-12 receptor deficiency. Science **280:**1432–1435. http://dx.doi.org/10.1126/science.280.5368.1432.
7. **Junqueira-Kipnis AP, Kipnis A, Jamieson A, Juarrero MG, Diefenbach A, Raulet DH, Turner J, Orme IM.** 2003. NK cells respond to pulmonary infection with *Mycobacterium tuberculosis*, but play a minimal role in protection. J. Immunol. **171:**6039–6045. http://dx.doi.org/10.4049/jimmunol.171.11.6039.
8. **Lebrun I, Marques-Porto R, Pereira A, Pereira A, Perpetuo E.** 2009. Bacterial toxins: an overview on bacterial proteases and their action as virulence factors. Mini Rev. Med. Chem. **9:**820–828. http://dx.doi.org/10.2174/138955709788452603.
9. **Master SS, Rampini SK, Davis AS, Keller C, Ehlers S, Springer B, Timmins GS, Sander P, Deretic V.** 2008. *Mycobacterium tuberculosis* prevents inflammasome activation. Cell Host Microbe **3:**224–232. http://dx.doi.org/10.1016/j.chom.2008.03.003.
10. **Yanagisawa M, Kurihara H, Kimura S, Tomobe Y, Kobayashi M, Mitsui Y, Yazaki Y, Goto K, Masaki T.** 1988. A novel potent vasoconstrictor peptide produced by vascular endothelial cells. Nature **332:**411–415. http://dx.doi.org/10.1038/332411a0.
11. **Comellas AP, Briva A.** 2009. Role of endothelin-1 in acute lung injury. Transl. Res. **153:**263–271. http://dx.doi.org/10.1016/j.trsl.2009.02.007.
12. **Barton M, Yanagisawa M.** 2008. Endothelin: 20 years from discovery to therapy. Can. J. Physiol. Pharmacol. **86:**485–498. http://dx.doi.org/10.1139/Y08-059.
13. **Kedzierski RM, Yanagisawa M.** 2001. Endothelin system: the double-edged sword in health and disease. Annu. Rev. Pharmacol. Toxicol. **41:**851–876. http://dx.doi.org/10.1146/annurev.pharmtox.41.1.851.
14. **Nett PC, Teixeira MM, Candinas D, Barton M.** 2006. Recent developments on endothelin antagonists as immunomodulatory drugs–from infection to transplantation medicine. Recent Pat. Cardiovasc. Drug Discov. **1:**265–276. http://dx.doi.org/10.2174/157489006778776990.
15. **Jandeleit-Dahm KAM, Watson AMD.** 2012. The endothelin system and endothelin receptor antagonists. Curr. Opin. Nephrol. Hypertens. **21:**66–71. http://dx.doi.org/10.1097/MNH.0b013e32834dde48.
16. **Tanowitz HB, Huang H, Jelicks LA, Chandra M, Loredo ML, Weiss LM, Factor SM, Shtutin V, Mukherjee S, Kitsis RN, Christ GJ, Wittner M, Shirani J, Kisanuki YY, Yanagisawa M.** 2005. Role of endothelin 1 in the pathogenesis of chronic chagasic heart disease. Infect. Immun. **73:**2496–2503. http://dx.doi.org/10.1128/IAI.73.4.2496-2503.2005.
17. **Corral RS, Guerrero NA, Cuervo H, Gironès N, Fresno M.** 2013. *Trypanosoma cruzi* infection and endothelin-1 cooperatively activate pathogenic inflammatory pathways in cardiomyocytes. PLoS Negl. Trop. Dis. **7:**e2034. http://dx.doi.org/10.1371/journal.pntd.0002034.
18. **Chauhan A, Hahn S, Gartner S, Pardo CA, Netesan SK, McArthur J, Nath A.** 2007. Molecular programming of endothelin-1 in HIV-infected brain: role of Tat in up-regulation of ET-1 and its inhibition by statins. FASEB J. **21:**777–789. http://dx.doi.org/10.1096/fj.06-7054com.
19. **Ehrenreich H, Rieckmann P, Sinowatz F, Weih KA, Arthur LO, Goebel FD, Burd PR, Coligan JE, Clouse KA.** 1993. Potent stimulation of monocytic endothelin-1 production by HIV-1 glycoprotein 120. J. Immunol. **150:**4601–4609.
20. **Hebert VY, Crenshaw BL, Romanoff RL, Ekshyyan VP, Dugas TR.** 2004. Effects of HIV drug combinations on endothelin-1 and vascular cell proliferation. Cardiovasc. Toxicol. **4:**117–131. http://dx.doi.org/10.1385/CT:4:2:117.

21. **Fernandes LB, D'Aprile AC, Self GJ, Harnett GB, Goldie RG.** 2004. The impact of respiratory syncytial virus infection on endothelin receptor function and release in sheep bronchial explants. J. Cardiovasc. Pharmacol. **44**(Suppl 1)**:**S202–S206. http://dx.doi.org/10.1097/01.fjc.0000166236.57077.9f.
22. **Knott PG, Henry PJ, McWilliam AS, Rigby PJ, Fernandes LB, Goldie RG.** 1996. Influence of parainfluenza-1 respiratory tract viral infection on endothelin receptor-effector systems in mouse and rat tracheal smooth muscle. Br. J. Pharmacol. **119:**291–298. http://dx.doi.org/10.1111/j.1476-5381.1996.tb15984.x.
23. **Schuetz P, Stolz D, Mueller B, Morgenthaler NG, Struck J, Mueller C, Bingisser R, Tamm M, Christ-Crain M.** 2008. Endothelin-1 precursor peptides correlate with severity of disease and outcome in patients with community acquired pneumonia. BMC Infect. Dis. **8:**22. http://dx.doi.org/10.1186/1471-2334-8-22.
24. **Wessel D, Flügge UI.** 1984. A method for the quantitative recovery of protein in dilute solution in the presence of detergents and lipids. Anal. Biochem. **138:**141–143. http://dx.doi.org/10.1016/0003-2697(84)90782-6.
25. **Gonzalez-Juarrero M, Shim TS, Kipnis A, Junqueira-Kipnis AP, Orme IM.** 2003. Dynamics of macrophage cell populations during murine pulmonary tuberculosis. J. Immunol. **171:**3128–3135. http://dx.doi.org/10.4049/jimmunol.171.6.3128.
26. **Bourque SL, Davidge ST, Adams MA.** 2011. The interaction between endothelin-1 and nitric oxide in the vasculature: new perspectives. Am. J. Physiol. Regul. Integr. Comp. Physiol. **300:**R1288–R1295. http://dx.doi.org/10.1152/ajpregu.00397.2010.
27. **Yang C-S, Yuk J-M, Jo E-K.** 2009. The role of nitric oxide in mycobacterial infections. Immune Netw. **9:**46–52. http://dx.doi.org/10.4110/in.2009.9.2.46.
28. **Gabrilovich DI, Nagaraj S.** 2009. Myeloid-derived suppressor cells as regulators of the immune system. Nat. Rev. Immunol. **9:**162–174. http://dx.doi.org/10.1038/nri2506.
29. **Petrera A, Amstutz B, Gioia M, Hähnlein J, Baici A, Selchow P, Ferraris DM, Rizzi M, Sbardella D, Marini S, Coletta M, Sander P.** 2012. Functional characterization of the *Mycobacterium tuberculosis* zinc metallopeptidase Zmp1 and identification of potential substrates. Biol. Chem. **393:**631–640. http://dx.doi.org/10.1515/hsz-2012-0106.
30. **Froeliger EH, Oetjen J, Bond JP, Fives-Taylor P.** 1999. *Streptococcus parasanguis pepO* encodes an endopeptidase with structure and activity similar to those of enzymes that modulate peptide receptor signaling in eukaryotic cells. Infect. Immun. **67:**5206–5214.
31. **Oetjen J, Fives-Taylor P, Froeliger E.** 2001. Characterization of a streptococcal endopeptidase with homology to human endothelin-converting enzyme. Infect. Immun. **69:**58–64. http://dx.doi.org/10.1128/IAI.69.1.58-64.2001.
32. **Carson JA, Ansai T, Awano S, Yu W, Takehara T, Turner AJ.** 2002. Characterization of PgPepO, a bacterial homologue of endothelin-converting enzyme-1. Clin. Sci. **103**(Suppl 48)**:**90S–93S.
33. **Awano S, Ansai T, Mochizuki H, Yu W, Tanzawa K, Turner AJ, Takehara T.** 1999. Sequencing, expression and biochemical characterization of the *Porphyromonas gingivalis* pepO gene encoding a protein homologous to human endothelin-converting enzyme. FEBS Lett. **460:**139–144. http://dx.doi.org/10.1016/S0014-5793(99)01326-5.
34. **Kok J, Mierau I, Monnet V.** 2013. Chapter 136. Oligopeptidase O, p 650–653. *In* Rawlings ND, Salvesen G (ed), Handbook of proteolytic enzymes. Academic Press, New York, NY.
35. **Ferraris DM, Sbardella D, Petrera A, Marini S, Amstutz B, Coletta M, Sander P, Rizzi M.** 2011. Crystal structure of *Mycobacterium tuberculosis* zinc-dependent metalloprotease-1 (Zmp1), a metalloprotease involved in pathogenicity. J. Biol. Chem. **286:**32475–32482. http://dx.doi.org/10.1074/jbc.M111.271809.
36. **Kimura S, Kasuya Y, Sawamura T, Shinmi O, Sugita Y, Yanagisawa M, Goto K, Masaki T.** 1988. Structure-activity relationships of endothelin: importance of the C-terminal moiety. Biochem. Biophys. Res. Commun. **156:**1182–1186. http://dx.doi.org/10.1016/S0006-291X(88)80757-5.
37. **Douglas SA, Hiley CR.** 1991. Endothelium-dependent mesenteric vasorelaxant effects and systemic actions of endothelin (16-21) and other endothelin-related peptides in the rat. Br. J. Pharmacol. **104:**311–320. http://dx.doi.org/10.1111/j.1476-5381.1991.tb12428.x.
38. **Schmidtchen A, Frick I-M, Andersson E, Tapper H, Björck L.** 2002. Proteinases of common pathogenic bacteria degrade and inactivate the antibacterial peptide LL-37. Mol. Microbiol. **46:**157–168. http://dx.doi.org/10.1046/j.1365-2958.2002.03146.x.
39. **Beauvais A, Monod M, Wyniger J, Debeaupuis JP, Grouzmann E, Brakch N, Svab J, Hovanessian AG, Latge JP.** 1997. Dipeptidyl-peptidase IV secreted by *Aspergillus fumigatus*, a fungus pathogenic to humans. Infect. Immun. **65:**3042–3047.
40. **Bastos I, Motta F, Grellier P, Santana J.** 2013. Parasite prolyl oligopeptidases and the challenge of designing chemotherapeuticals for Chagas disease, leishmaniasis and African trypanosomiasis. Curr. Med. Chem. **20:**3103–3115. http://dx.doi.org/10.2174/09298673113202500006.
41. **Johansen P, Fettelschoss A, Amstutz B, Selchow P, Waeckerle-Men Y, Keller P, Deretic V, Held L, Kündig TM, Böttger EC, Sander P.** 2011. Relief from Zmp1-mediated arrest of phagosome maturation is associated with facilitated presentation and enhanced immunogenicity of mycobacterial antigens. Clin. Vaccine Immunol. **18:**907–913. http://dx.doi.org/10.1128/CVI.00015-11.
42. **Fabricio ASC, Rae GA, Zampronio AR, D'Orléans-Juste P, Souza GEP.** 2006. Central endothelin ETB receptors mediate IL-1-dependent fever induced by preformed pyrogenic factor and corticotropin-releasing factor in the rat. Am. J. Physiol. **290:**R164–R171. http://dx.doi.org/10.1152/ajpregu.00337.2005.
43. **Pedrosa J, Saunders BM, Appelberg R, Orme IM, Silva MT, Cooper AM.** 2000. Neutrophils play a protective nonphagocytic role in systemic *Mycobacterium tuberculosis* infection of mice. Infect. Immun. **68:**577–583. http://dx.doi.org/10.1128/IAI.68.2.577-583.2000.
44. **Obregón-Henao A, Henao-Tamayo M, Orme IM, Ordway DJ.** 2013. Gr1(int)CD11b+ myeloid-derived suppressor cells in *Mycobacterium tuberculosis* infection. PLoS One **8:**e80669. http://dx.doi.org/10.1371/journal.pone.0080669.
45. **Du Plessis N, Loebenberg L, Kriel M, von Groote-Bidlingmaier F, Ribechini E, Loxton AG, van Helden PD, Lutz MB, Walzl G.** 2013. Increased frequency of myeloid-derived suppressor cells during active tuberculosis and after recent *Mycobacterium tuberculosis* infection suppresses T-cell function. Am. J. Respir. Crit. Care Med. **188:**724–732. http://dx.doi.org/10.1164/rccm.201302-0249OC.
46. **MacLean MR, McCulloch KM, Baird M.** 1994. Endothelin ETA- and ETB-receptor-mediated vasoconstriction in rat pulmonary arteries and arterioles. J. Cardiovasc. Pharmacol. **23:**838–845. http://dx.doi.org/10.1097/00005344-199405000-00022.
47. **De Nucci G, Thomas R, D'Orleans-Juste P, Antunes E, Walder C, Warner TD, Vane JR.** 1988. Pressor effects of circulating endothelin are limited by its removal in the pulmonary circulation and by the release of prostacyclin and endothelium-derived relaxing factor. Proc. Natl. Acad. Sci. U. S. A. **85:**9797–9800. http://dx.doi.org/10.1073/pnas.85.24.9797.
48. **Hasunuma K, Rodman DM, O'Brien RF, McMurtry IF.** 1990. Endothelin 1 causes pulmonary vasodilation in rats. Am. J. Physiol. **259:**H48–H54.
49. **Lüscher TF, Barton M.** 2000. Endothelins and endothelin receptor antagonists: therapeutic considerations for a novel class of cardiovascular drugs. Circulation **102:**2434–2440. http://dx.doi.org/10.1161/01.CIR.102.19.2434.
50. **Griswold DE, Douglas SA, Martin LD, Davis TG, Davis L, Ao Z, Luttmann MA, Pullen M, Nambi P, Hay DW, Ohlstein EH.** 1999. Endothelin B receptor modulates inflammatory pain and cutaneous inflammation. Mol. Pharmacol. **56:**807–812.
51. **Imhof A-K, Glück L, Gajda M, Bräuer R, Schaible H-G, Schulz S.** 2011. Potent anti-inflammatory and antinociceptive activity of the endothelin receptor antagonist bosentan in monoarthritic mice. Arthritis Res. Ther. **13:**R97. http://dx.doi.org/10.1186/ar3372.
52. **Fabricio ASC, Silva CAA, Rae GA, D'Orleans-Juste P, Souza GEP.** 1998. Essential role for endothelin ETB receptors in fever induced by LPS (*E. coli*) in rats. Br. J. Pharmacol. **125:**542–548. http://dx.doi.org/10.1038/sj.bjp.0702075.
53. **Subbian S, Bandyopadhyay N, Tsenova L, O Brien P, Khetani V, Kushner NL, Peixoto B, Soteropoulos P, Bader JS, Karakousis PC, Fallows D, Kaplan G.** 2013. Early innate immunity determines outcome of *Mycobacterium tuberculosis* pulmonary infection in rabbits. Cell Commun. Signal. **11:**60. http://dx.doi.org/10.1186/1478-811X-11-60.
54. **Liu S, Premont RT, Kontos CD, Huang J, Rockey DC.** 2003. Endothelin-1 activates endothelial cell nitric-oxide synthase via heterotrimeric G-protein betagamma subunit signaling to protein jinase B/Akt. J. Biol. Chem. **278:**49929–49935. http://dx.doi.org/10.1074/jbc.M306930200.
55. **Herrera M, Hong NJ, Ortiz PA, Garvin JL.** 2009. Endothelin-1 inhibits thick ascending limb transport via Akt-stimulated nitric oxide

production. J. Biol. Chem. **284:**1454–1460. http://dx.doi.org/10.1074/jbc.M804322200.
56. **Razavi HM, Wang LF, Weicker S, Rohan M, Law C, McCormack DG, Mehta S.** 2004. Pulmonary neutrophil infiltration in murine sepsis: role of inducible nitric oxide synthase. Am. J. Respir. Crit. Care Med. **170:**227–233. http://dx.doi.org/10.1164/rccm.200306-846OC.
57. **MacMicking JD, North RJ, LaCourse R, Mudgett JS, Shah SK, Nathan CF.** 1997. Identification of nitric oxide synthase as a protective locus against tuberculosis. Proc. Natl. Acad. Sci. U. S. A. **94:**5243–5248. http://dx.doi.org/10.1073/pnas.94.10.5243.
58. **Boshoff HIM, Barry CE, III.** 2005. Tuberculosis–metabolism and respiration in the absence of growth. Nat. Rev. Microbiol. **3:**70–80. http://dx.doi.org/10.1038/nrmicro1065.
59. **Aly S, Wagner K, Keller C, Malm S, Malzan A, Brandau S, Bange F-C, Ehlers S.** 2006. Oxygen status of lung granulomas in *Mycobacterium tuberculosis*-infected mice. J. Pathol. **210:**298–305. http://dx.doi.org/10.1002/path.2055.
60. **Tsai MC, Chakravarty S, Zhu G, Xu J, Tanaka K, Koch C, Tufariello J, Flynn J, Chan J.** 2006. Characterization of the tuberculous granuloma in murine and human lungs: cellular composition and relative tissue oxygen tension. Cell. Microbiol. **8:**218–232. http://dx.doi.org/10.1111/j.1462-5822.2005.00612.x.